Research Academy for Young Scientists

Investigating the Efficacy and Duration of siRNA Knockdown of Key Regulatory Genes in Adult Neural Stem Cells

Jack Elliot Collier Ryder
jack.collier.ryder@gmail.com

under the direction of
Ruxandra Covacu, Ph.D.
Karolinska Institute
Department of Clinical Neuroscience

July 12, 2023

*

Abstract

A multitude of factors impact a neural stem cell's tendency to differentiate or proliferate, and one example is regulatory genes. This study examined the efficacy and duration of gene knockdown induced by siRNA transfection in neural stem cells for the regulatory genes FoxO1 and Hes1. siRNA is a commonly used perturbation technique that can help explore the involvement of a gene in a biological process. Examining specific gene knockdown efficacy and duration for siRNAs which are used in a study is important for confirmation of validity. In this study, first a transfection of NSCs using siRNA was performed. The transfection was followed by isolation after 24 and 48 hours depending on the sample. That was followed by an analysis of the gene expression with RT-qPCR. The study concluded that the siHes1 obtained a relative gene fold of approximately 47% and 49% efficacy after 24 and 48 hours respectively. The siFoxo1 knockdown efficacy of the Foxo1 gene was approximately 52% after 24 hours and 56% after 48 hours. This means that both transfections were successful. Moreover, no significant differences were observed between 24 and 48 hours for any of the samples. The understanding of the knockdown of these genes might be used to further the development of treatments for neurodegenerative diseases like multiple sclerosis.

Acknowledgements

I would like to begin with expressing the utmost of gratitude to my mentor, Ruxandra Covacu, Ph.D. for answering my countless questions and being a fantastic guide through the realm of molecular biology. I would also like to thank the Center for Molecular Biology at the Karolinska Institute for enabling this opportunity.

I would also like to express my appreciation to everyone in the organisation of Rays - for Excellence. Because of them, young aspiring scientists get to truly delve into advanced projects, which is an absolutely incredible opportunity. I would also like to thank all the people I have gotten to know here during Rays who have been incredibly supportive during the entire process. A special thanks goes out the the people who took the time to read through this report and help me improve it.

Finally, I would like to extend my appreciation to Rays - for Excellence collaborative partners *AstraZeneca* and *Magn. Bergvalls stiftelse* for making this incredible opportunity possible.

Contents

1 Introduction

Neural stem cells (NSC) are fundamental components during the development of a human's nervous system. Contrary to a notion that prevailed until the end of the 20th century, they remain in the nervous system and differentiate into specialized cells throughout a person's entire life. Moreover, learning to understand these cells can be essential for curing cognitive disorders and improving the lives of countless people. [1]

1.1 Theoretical Background

NSCs have been studied for more than 50 years and still undertake a lot of complex behavior which is not fully understood in homeostasis, and even less so when the central nervous system (CNS) is under stress. [2]

1.1.1 Neural Stem Cells

The human brain is one of the most complex organs and an elucidation of the underlying intricacies is the existence of an estimated 100 trillion synaptic connections [3]. The brain, together with the spinal cord, constitutes the CNS. The formation of the CNS starts with the ectoderm, which gives rise to the neural ectoderm, which further develops into the neural tube and the neural crest, which over time gives rise to the entire nervous system [4]. The components which instigate the development are NSCs, and previous studies have indicated that the NSCs active during embryonic development divide either symmetrically or asymmetrically [5]. Symmetric division implies increasing the number of NSCs and asymmetric division means giving rise to either intermediate progenitor cells (IPCs) or differentiating to neurons, oligodendrocytes, or astrocytes [6].

Neurons, oligodendrocytes, and astrocytes consequently make up the CNS, and a long-held belief was that CNS development ceased in adulthood. In contrast to this belief, during the past decades, a consensus has flourished that neurogenesis occurs throughout a human's life due to a continued prevalence of NSCs [7]. In the adult brain, active NSCs, exist in two primary locations; the subventricular zone lining the lateral ventricles and the subgranular zone in the dentate gyrus of the hippocampus [8]. Additionally, quiescent

NSCs exist in the spinal cord. [9]

Adult NSCs in the subventricular zone (type B cells) showcase astrocytic characteristics and extend an apical process contacting the cerebrospinal fluid and a basal process contacting the blood vessels. Type B cells further engender the formation of transient amplifying progenitors, which in turn develop into neuroblasts which migrate into the olfactory bulb from where they migrate radially, differentiating into interneurons [10]. In the subgranular zone, radial glial-like cells give rise to intermediate progenitor cells which proliferate a finite amount before instigating the creation of neuroblasts which further develop into immature neurons and subsequently dentate granule neurons. [8]

Multiple factors impact NSCs' inclination to differentiate or proliferate, and one such factor is the prevalence of key regulatory genes. [11]. Understanding how these genes work and react to external stimuli can be crucial for developing a deeper understanding of NSCs. Examples of key regulatory genes are hairy and enhancer of split-1 (Hes1) and forkhead transcription factor family O (FoxO) which both increase NSCs' tendency to proliferate and decrease their tendency to differentiate [12] [13].

1.1.2 Multiple Sclerosis

Multiple sclerosis (MS) is a chronic autoimmune disorder characterized by the immune system's T-cells, B-cells, and macrophages degradation of myelin sheaths surrounding the axons of neurons [14]. The accumulation of astrogliosis, demyelination, and subsequential deterioration of neurons give rise to CNS plaques that result in cognitive deficits. Symptoms depend on the lesion's location but common symptoms include vision impairment, reduced cognitive ability, and chronic fatigue. The precise pathogenesis is unknown [15]. However, it is believed to be caused by genetic factors and environmental triggers which can result in the initiation of the disorder. Possible environmental factors which impact the risk of MS are smoking, Epstein-Barr virus, and high latitude [16]. Relapsing remitting MS is the most common variation, appearing in an estimated 85% of cases. What distinguishes relapsing remitting MS is that it consists of flare-ups signified by worsened symptoms separated by periods of improvement. In the case of flare-ups, NSCs can pro-

vide an anti-inflammatory effect as well as providing trophic support to surrounding tissue [17]. In addition to this, oligodendrocytes cause remyelination of the axons, giving rise to the question of whether NSCs could be used to develop treatments for MS and other neurodegenerative disorders. [1]

1.2 Background to the Method

To analyze the regulatory genes, a method consisting of transfection of small interfering ribonucleic acid, isolation of RNA, and quantitative reverse transcription polymerase chain reaction (RT-qPCR) was used. This section explains the theoretical background to the steps in the method.

1.2.1 siRNA Transfection

Transfection of siRNA is a method used for gene silencing and siRNA are small RNAs which have the ability to degrade mRNA and consequently silence particular genes. After the transfection of siRNA, first an enzyme of the family RNase III named Dicer binds to dsRNA dividing the strand into 20-25 nucleotide strands containing nucleotide overhangs of atypical length on both the 3' and 5' end [18]. The strand with the less thermodynamically stable 5' end, is incorporated into an RNA-induced silencing complex (RISC) to target RNA [19]. The other strand is degraded by RISC. siRNA can be made targeting almost any gene, and in this study, the following siRNA stocks were used: siNTC, siHes1, siFoxO1, and siTcf712 [20]. Moreover, RISC consists of an Argonaute protein (Ago2) which is the catalytically active RNase in RISC and is, therefore, the part which degrades mRNA and consequently prohibits translation of protein [21]. A visual interpretation of RISC formation and application can be found in Figure 1b.

For transfection of siRNA a transfection reagent is used to deliver the nucleic acids into the eukaryotic cells [22]. Lipofectamine operates using liposome-mediated transfection, which means that the RNA forms a lipoplex together with a cationic liposome. The lipoplex is absorbed into the cell through endocytosis due to the liposomes' similarities to the cell membrane. The siRNA then initiates degradation of mRNA, causing gene

silencing. A simplified depiction can be found in Figure 1a. [23]

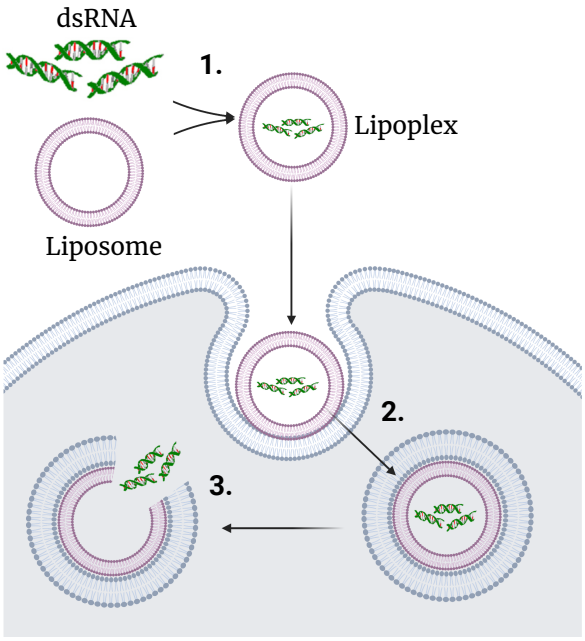

(a) Schematic depiction of transfection:
1. Formation of lipoplex by siRNA and liposome with lipid bilayer
2. Endocytosis of lipoplex due to similarities
3. Depletion of lipoplex, emancipating siRNA

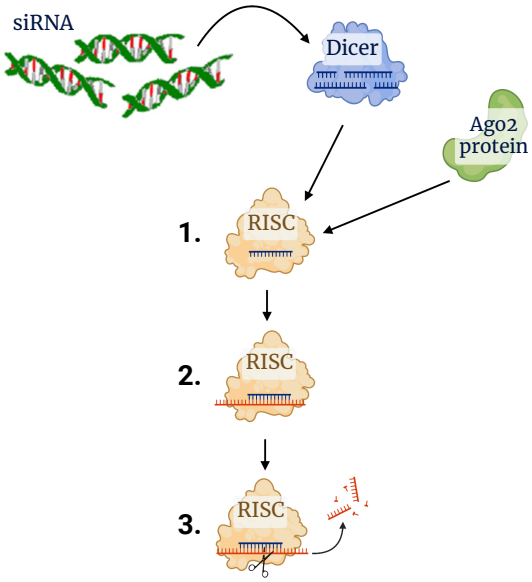

(b) Schematic depiction of RISC formation:
1. siRNA forming RISC with Dicer and an Argonaute protein.
2. RISC finding mRNA which binds to siRNA
3. Argonaute protein degrades mRNA

Figure 1: Simplified visualizations of siRNA transfected into a cell and siRNA degrading mRNA inhibiting translation in turn silencing the gene.

Created with BioRender.com
Courtesy of eurofins Genomics

1.2.2 RNA Isolation using TRIzol

TRIzol™, consisting of phenol and guanidinium isothiocyanate, causes lysis which entails degradation of the cell, but maintainence of the structural integrity of the RNA. Chloroform instigates a phase separation, a bottom organic phase containing proteins and lipids, an interphase containing DNA, and a top aqueous phase where RNA resides. In the case of RNA isolation, the supernatant is extracted and the bottom two layers are discarded. Isopropanol precipitates the RNA, creating a pellet and the glycogen-based GlycoBlue Coprecipitant [24] dyes the RNA pellet blue for easier extraction. [25]

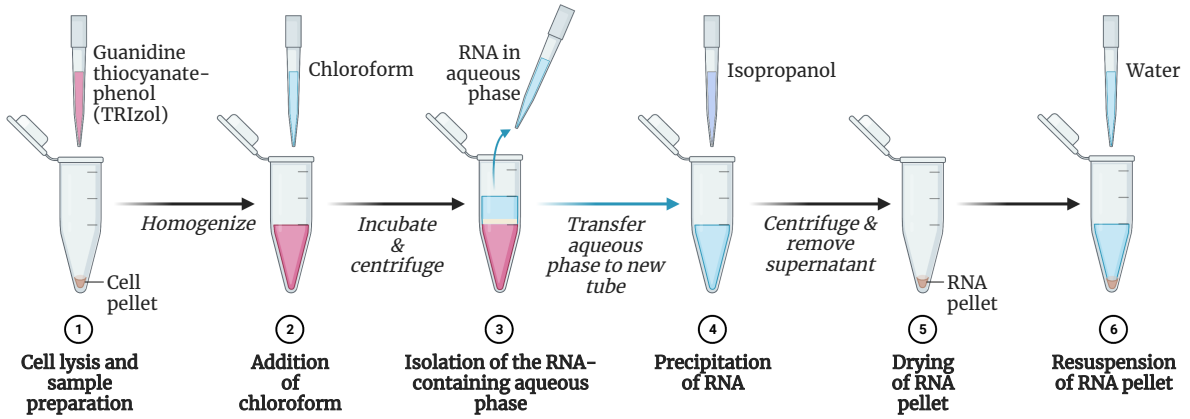

Figure 2: Schematic explanation of RNA extraction process using TRIzol

Created with BioRender.com

Contamination of isolated RNA can be detected by a nanodrop spectrophotometer. The absorbed wavelength of the strand depends on the composition of the object and generally, the absorbance at 260 nm indicates nucleotides, 280 nm indicate proteins or phenol and 230 nm carbohydrates and phenol. The desired ratio for 260/280 is 2.0 and 260/230 is 2.0-2.2. [26]

1.2.3 RT-qPCR

To determine gene expression levels, RT-qPCR can be used. Reverse Transcription (RT) which turns RNA into complementary DNA (cDNA) is performed since DNA is more stable than RNA during analysis. During RT, either random hexamer primers are used or oligo-dT primers which attach to the 3' poly-A tail of the strand. The RNA-dependent DNA polymerase, reverse transcriptase then attaches to the primer and performs synthesis of the complementary DNA strand. [27]

PCR, which exponentially amplifies the amount of DNA can be used for determining gene expression. A simplified exemplification of the PCR process is shown in Figure 4. The reaction process begins with the denaturation phase, where the dsDNA is denatured and made single stranded. Secondly, during the annealing phase, the DNA is cooled and around 20 nucleotide long primers anneal to the strands. Finally, the primers on both strands are elongated from the 5' to the 3' end by polymerase activity. [28]

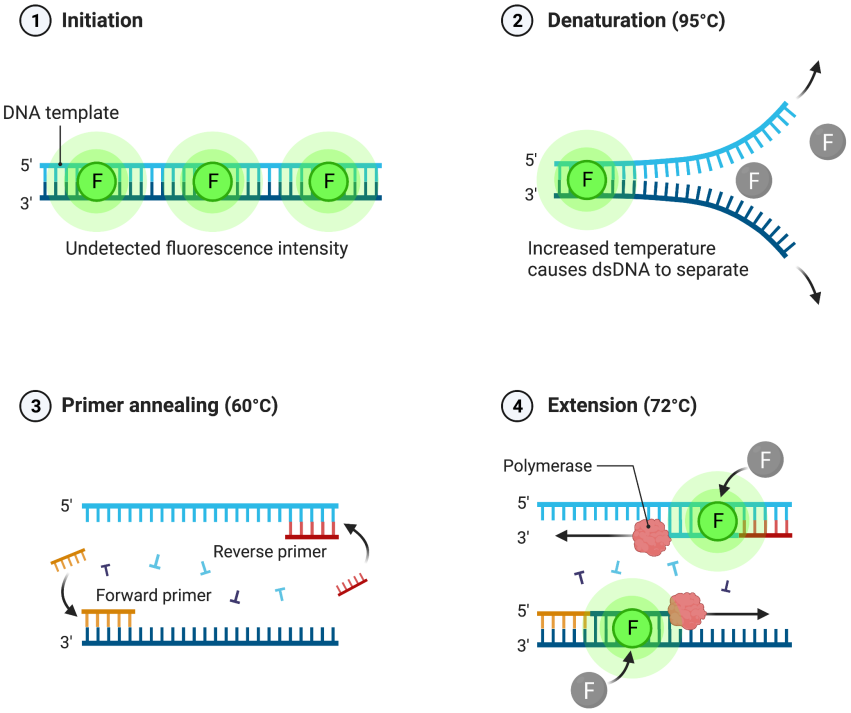

Figure 3: Schematic explanation of 4 major steps for qPCR using fluorescent dye.

Adapted from "Fluorescent Dye-Based Real Time PCR (qPCR) 4 Steps", by BioRender.com (2023). Retrieved from BioRender.com/biorender-templates

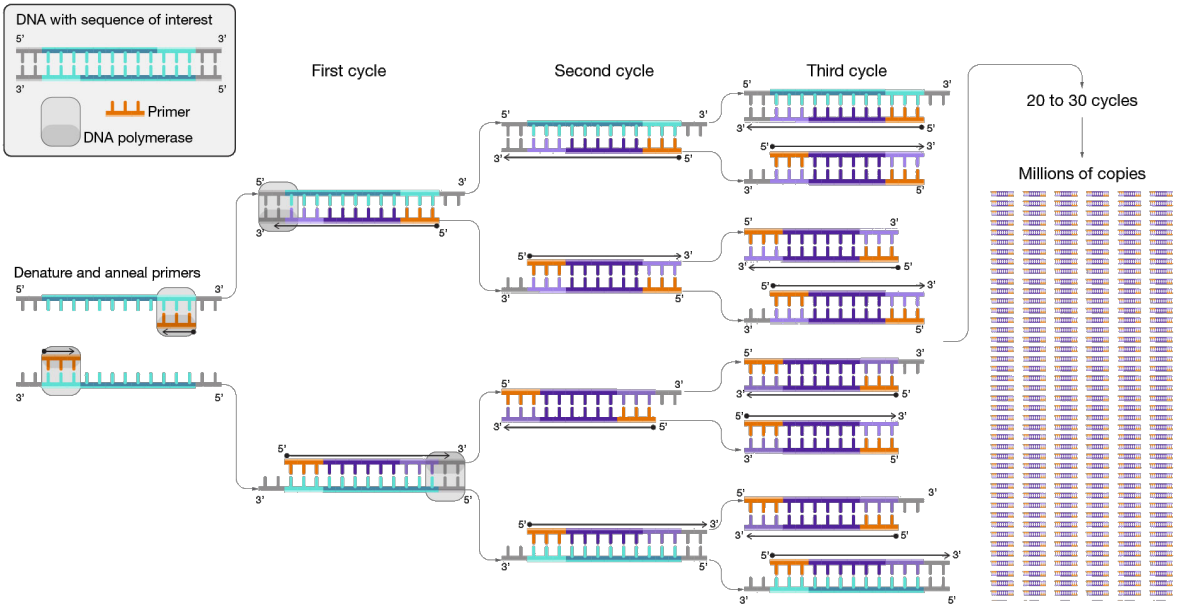

Figure 4: Schematic interpretation of PCR amplification

Courtesy: National Human Genome Research Institute

In practice, PCR graphs attain a sigmoidal shape which consists of an initial baseline value, a subsequent linear-log phase, and a final plateau. Initially, reagents are not limiting and the amount of generated product is small but after an accumulation of pyrophosphates and a self-annealing of product causes the reaction efficiency to decrease [29]. This implies that extrapolating an absolute quantification of the initial value from the endpoint value is unreliable. Therefore, real-time PCR (qPCR) which tracks the DNA amplification in real-time, is used [30]. The foremost distinction is qPCR's inclusion of a fluorescent assay like SYBR Green I. SYBR Green I is an asymmetrical cyanine dye that binds to the minor groove of dsDNA absorbing blue light ($\lambda_{max} = 497\,\text{nm}$) and emitting green light ($\lambda_{max} = 525\,\text{nm}$). The accumulated fluorescence is examined after each PCR cycle by a fluorometer. [31]

The quantification cycle (C_q) signifies when the fluorescence is more substantial than the background level. The C_q values contain no intrinsic comparative quantitative value due to alterations between qPCRs. A relative expression is therefore used, comparing the expression to a housekeeping gene which is constitutively expressed, serving as a benchmark. A commonly used housekeeping gene is Actin [28]. Relative expression is determined by

$$\text{Relative Expression} = 2^{-\Delta C_q} \tag{1}$$

where $\Delta\text{C}_q = \text{C}_q$ of a target gene - C_q of the housekeeping gene in the same sample. Each experimental condition that is investigated can be further normalized to its control. The delta-delta C_t method is used to determine the relative fold change in expression relative to the control according to

$$\text{delta-delta C}_q = 2^{-\Delta\Delta C_q} \tag{2}$$

where $\Delta\Delta C_q = \Delta\text{C}_q(\text{treated}) - \Delta\text{C}_q(\text{untreated})$. [31]

Standard curves correlate the concentration of each sample from a dilution series to a C_q value. Analysing the data can assure that differences between control and target samples is due to different quantities of target gene, and not PCR efficiency in the different samples. The curve's slope can be used to determine a theoretical geometric PCR

efficiency, calculated by the equation

$$e = 10^{-1/\text{slope}} \tag{3}$$

which implies that a slope of approximately -3.32 attains a value of 2.0 and is consequently 100% effective [32]. Ideally the slope resides in the interval -3.6 $>$ slope $>$ -3.3 inferring an efficiency of 90-100%. [33]

Since intercalating dyes are not sequence-specific, but bind to any dsDNA, the strands are heated and the reduction of fluorescence while the strands denature is analyzed. Different sequences attain dissimilar melting points based on the content of Guanine-Cytosine bonds relative to the amount of Adenine-Thymine bonds. Accordingly, if a PCR sample consists of many DNA sequences, abrupt decreases in fluorescence will appear at several time points during an analysis of the melting. In addition to this, inconsistencies in melting curve peaks can be caused by primer dimers. [28]

1.3 Previous Studies

Studies examining the siRNA knockdown efficacy and duration of a type of cells called HeLa cells have shown that the siRNA knockdown maintains at almost maximal knockdown for 5-7 days. Generally, protocols suggest transfecting between 24 and 48 hours, however, due to deviations between genes, the actual duration and efficacy must be tested for every gene which is going to be used. [34]

A study examining the gene knockdown of several different genes using Invitrogen Lipofectamine RNAiMAX Transfection Reagent in human embryonic stem cells (hES) was conducted [23]. The study displayed that the reagent could reduce the gene expression of Sox2 by 71% and that the expression of Oct4 was downregulated by 90%. Moreover, a study [35] was conducted analyzing the transfection efficacy of mouse adult neural stem cells achieved by electroporation. The study initially attained transfection rates between 40 and 77%, however when further optimizing the method achieved a transfection higher than 80%.

1.4 Aim of Study

Isolating how specific genes influence cellular function is a sought-after process for understanding the human genome. By silencing individual genes and analyzing alterations in behavior, conclusions can be drawn regarding the gene's impact. However, different cells and genes fluctuate in propensity of being knocked down, and therefore examining the knockdown efficacy and duration for individual genes is essential to further regulate the genes for future studies. In this study, the gene knockdown efficacy and duration for the key regulatory genes FoxO1 and Hes1 in NSCs are investigated.

2 Method

To determine the knockdown efficacy and durations, first, biopsies of the lateral ventricles from rats were performed to isolate NSCs. After culturing with selective media promoting the growth of NSCs, neurospheres formed. The Neurospheres were split to prevent cell death and the cells were seeded to instigate growth, transfected using siRNA and the RNA was then isolated using TRIzol, converted into cDNA and thereafter analyzed using qPCR.

2.1 Splitting the Cells

Biopsies of the lateral ventricle from four separate rats were isolated and subventricular zone NSCs were extracted. The NSCs were passaged into single cells and cultured to generate neurospheres. The cells were added to tubes and washed with L-15 medium (Life Technologies). The tubes were thereafter centrifuged at 230 RCF for 5 min and the supernatant was subsequently discarded. The cells were transfered to 15 mL tubes and 10 mL L-15 was added. The tubes were centrifuged, the supernatant was discarded and the cells were resuspended. Papain (Worthington/BioNordika) was heated to 37 °C and added to the tubes. In each tube, the cell suspension was pipetted up and down. The tubes were incubated three times at 37 °C for 5 min and between the incubations the cells were dissociated. Thereafter, 10 units of DNase were added to each tube per ml and the tubes

were incubated for 5 min. The cells were triturated and 0.5 mL BSA (Life technologies) and 10 mL L-15 were added to each sample. 10 µL from each tube was combined with an equal volume trypan blue (SigmaAldrich) and the cells were counted using a cell counter. The supernatant was thereafter discarded and the cells were resuspended. 900 µL culture medium consisting of the contents from Table 1 was added to each sample and solutions containing 100 000-200 000 cells were added to Petri dishes. The Petri dishes were then incubated for one week at 37 °C with 5 %CO_2.

2.2 Seeding the Cells

After the incubation of cells, the components from Table 1 were added to a Falcon tube, creating a master mix.

Table 1: Volume of components in master mix

Component	Quantity
DMEM/F-12 medium (Life technologies)	50 mL
B27 Supplement without Vitamin A (Life Technologies)	1 mL
Penicillin Streptomycin (Life technologies)	100 U/mL
Epidermal Growth Factor (mouse EGF, Sigma-Aldrich)	20 ng/mL
Human Basic Fibroblast Growth Factor (bFGF, R&D systems)	10 ng/mL

All solutions were diluted to 1 000 000 cells/mL and 75 µL was added to all 16 wells which were coated with poly D-lysine to cause the cells to stick to facilitate downstream analysis. 500 µL master mix was added to each well. The cells were incubated at 37 °C for 24 hours.

2.3 siRNA Transfection using Lipofectamine

The Invitrogen Lipofectamine RNAiMAX Transfection Reagent (Life Technologies) was followed. The medium in each well was exchanged for 450 µL of an identical medium except for the exclusion of penicillin-streptomycin.

A master mix was made containing 1000 µL Opti-MEM reduced serum medium (Gibco) and 60 µL lipofectamine transfection reagent (Invitrogen). Thereafter, four Eppendorf tubes were each filled with 250 µL Opti-MEM reduced serum medium and 5 µL of one of

the 10 µM siRNA stocks. An equal volume master mix was added to each sample. The solutions were mixed and incubated for 5 min at room temperature and subsequently, 50 µL of the siRNA reagent complex was added to each well containing cells. The plates were then transfected for 24 hours and in the 24-hour sample, the cells were harvested in TRIzol immediately after the transfection. In the 48-hour samples the mediums were exchanged to a propagation medium containing the same content excluding lipofectamine and the cells were harvested by TRIzol after an additional 24 hours.

2.4 RNA Isolation using TRIzol

To analyze the RNA, it needed to be isolated and the Ambion by Life Technologies TRIzol Reagent protocol was followed. First, the supernatant from each well was removed and replaced with 1 ml TRIzol (Invitrogen). After 2 min the contents of the wells were transferred to tubes. 200 µL chloroform was added to each tube and the tubes were flipped up and down continuously for 30 seconds. The lysates were then incubated for 3 min and were then centrifuged for 15 min at 5 °C and 12 000 RCF. A phase separation of the solution occurred and a the top phase was extracted into RNase-free tubes. 500 µL isopropanol was added to each tube followed by 3 µL glycogen. The solutions then precipitated for 10 minutes at room temperature. Thereafter, the tubes were centrifuged for 10 minutes at 12 000 RCF, the supernatant was discarded and 1 mL ethanol was added to each tube. For 1 hour, the tubes were chilled at 4 °C and were then centrifuged at 7500 RCF at 5 °C for 5 min. The supernatant was then discarded and the tubes were once again centrifuged at 7500 RCF at 5 °C for 1 min. The supernatant was discarded and the tubes were incubated at room temperature for 5 minutes. 25 µL RNase-free water was added to each tube to resuspend the RNA. The tubes were incubated for 10 min at 56 °C and a nanodrop spectrophotometer was thereafter used to calculate the RNA concentration and the 260/280 and 260/230 ratios for the samples.

2.5 Reverse Transcription for cDNA

When the RNA was isolated, The BIO RAD iScript cDNA Synthesis Kit protocol was followed to convert the RNA into cDNA. First 80 µL iScript Reaction Mix and 20 µL iScript reverse transcriptase was mixed forming a master mix. For every tube containing RNA, a new tube was filled with 5 µL master mix. Subsequently, a combined volume of 15 µL RNase-free water and the respective RNA was added to each tube. In the study, siTcf712 was excluded from the rest of the experiment. The ratio of water to RNA was dependent on the specific RNA concentration. The tube with the lowest RNA concentration consisted of only RNA, and the other samples were diluted so that they all contained equal amounts of RNA. The content of the tubes was transferred to 96-well plate which was inserted into a thermal cycler that followed the protocol found in Table 2.

Table 2: Procedure for thermal cycler for cDNA

Event	Time [min]	Temperature [°C]
Priming	5	25
Reverse Transcription	20	46
RT inactivation	1	95
Optional step	hold	4

The items were removed from the thermal cycler and stored at −20 °C

2.6 RT-qPCR

To prepare for analysis of the cDNA, 10 µL cDNA was transferred from 10 random wells to an Eppendorf tube. To determine the PCR efficiency at different DNA concentrations a 5-fold dilution series was made containing 4 tubes with 100 µL with the following dilutions: 1:1, 1:5, 1:25, and 1:125. The tubes were then frozen overnight and distributed into a 96-well plate. Reverse and forward primers for FoxO1, Hes1, and the housekeeping gene Actin were diluted to a concentration of 5 µM (Primer sequences can be found in Table 11 in the appendix). Subsequently, the components seen in Table 3 were added to an

Eppendorf tube for the respective primers.

Table 3: Master mix for qPCR

Component	Volume µL
SYBR Green I master mix (BIO-RAD)	195
5' primers	18
3' primers	18
dH_2O	159

13 µL master mix was added to a 384 well plate with 2 µL of the aforementioned diluted cDNAs. Technical duplicates were run for all cDNAs. In addition to this, two non template controls (NTC) were also added for every primer to provide an additional control for contamination of in the PCR mix, the primer dimers, or the genomic DNA. The plate was placed in the BIO-RAD PCR cycler and first, the PCR mix was preincubated for 2 min at 95 °C. The qPCR cycled through the program seen in Table 4, 40 times. Standard curves were then analyzed to assure that the qPCR procedure would work.

Table 4: Procedure for qPCR

Event	Time [s]	Temperature [°C]
Denaturation	30	95
Annealing of primers	30	60
Elongation	30	72

To analyze the various samples, a process identical to previous one was performed, except that each well was only filled with one specific RNA instead of a mix. This implied that for every gene and time point, two samples of every siRNA was used, as well as two NTCs and duplicates of every sample from the aforementioned dilution series. Table 5 shows the components for the master mix for each examined gene.

Table 5: Master mix for qPCR

Component	Volume [µL]
SYBR Green I master mix (BIO-RAD)	286
5' primers	26.4
3' primers	26.4
dH_2O	233.2

From the data obtained by the qPCR, standard curves were made examining the qPCR efficiency by optimizing a linear graph for the data points showcasing an inverted correlation between the dilution and the C_q. The R^2 and slope for the optimized graph were noted for each sample. Melting curves were also produced by increasing the temperature from 65 °C to 95 °C, incrementing 0.5 °C per cycle.

The qPCR curves were analyzed and the C_q was decided for each point by using the BIO-RAD CFX Maestro Software. ΔC_q, the expression level of each gene normalized to the housekeeping gene Actin with the same cDNA, and the relative fold expression normalized to the control siRNA was determined for each sample. The mean and resulting standard deviation of the relative expression were computed for each of the used siRNAs. The RM one-way ANOVA test was used to determine if there was a statistical significance denoted by $p<0.05$ between the sample's knockdown and the NTC control. The relative gene fold expression for the two time points for each of the different genes was calculated. Welch's t-test was used to determine if the values differed significantly from the mean.

3 Results

The cells were passaged and seeded. The exact concentration of the cell cultures and culture volume added to the Petri dish can be found in Table 7 in the appendix. The cells were split, and images thereof can be seen in Figure 5.

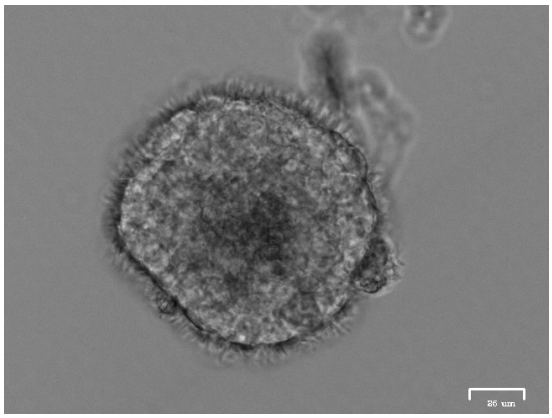

(a) Closeup of neurosphere which remained in cell culture despite cell splitting. The dark center showcases cell death due to insufficient nutrients in the center of the neurospheres.

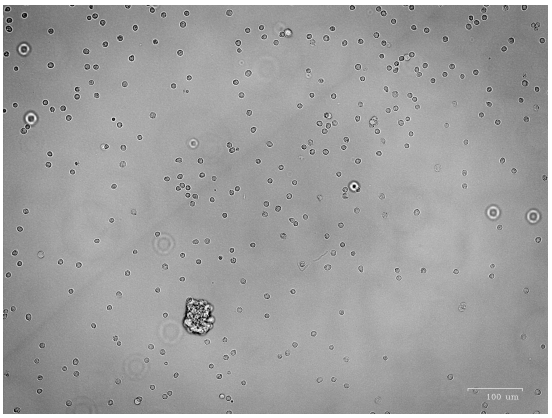

(b) NSCs show how most cells have separated from the neurospheres after splitting. The disassociation was not flawless, which is demonstrated by the relatively large neurosphere

Figure 5: Images of the cells after splitting

The RNA concentration determined by a nanodrop spectrophotometer and the volume to ensure an equal amount of RNA among samples is displayed in Table 8 and 9 for the 24 and 48 hour transfection group, respectively.

For the 24 hour samples, the nanodrop spectrphotometer estimated a mean 260/280 of ≈ 1.51 and the mean 260/230 to ≈ 0.43 (Table 10 in appendix). The qPCR amplification and standard curves showcasing approximate C_q for the samples as well as the PCR efficiency can be seen in Figure 6, 7 and 8.

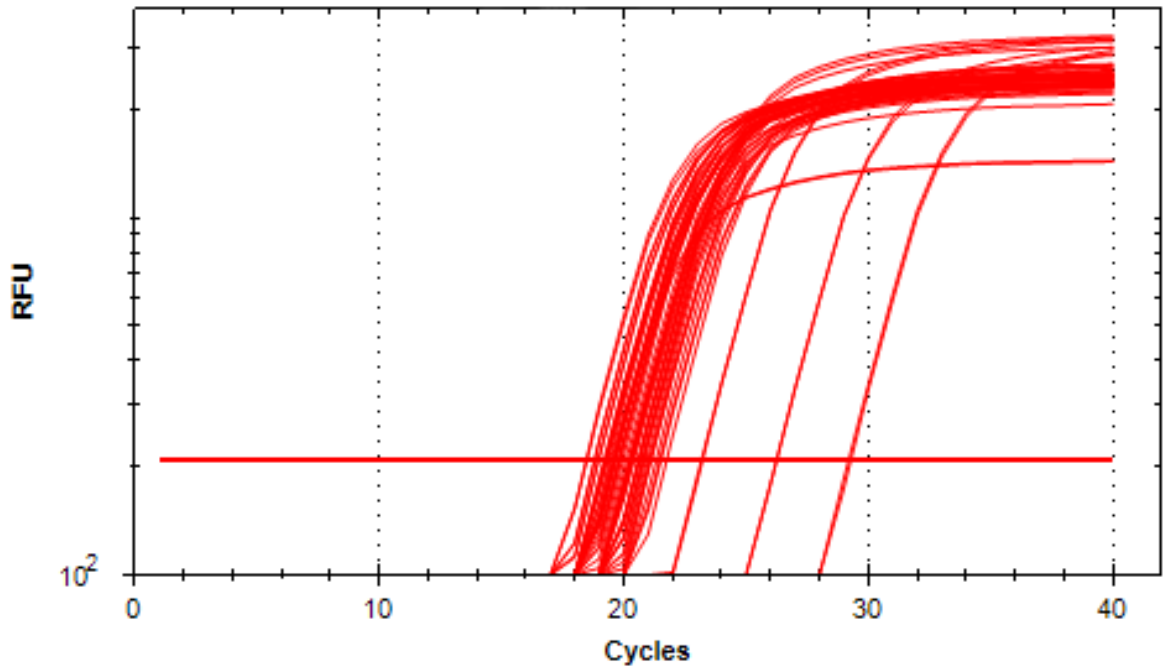

(a) Logarithmic amplification curve for PCR reaction containing Actin primers. Amount of cycles on the x-axis and relative fluorescence unit (RFU) on the y-axis. Threshold line also displayed

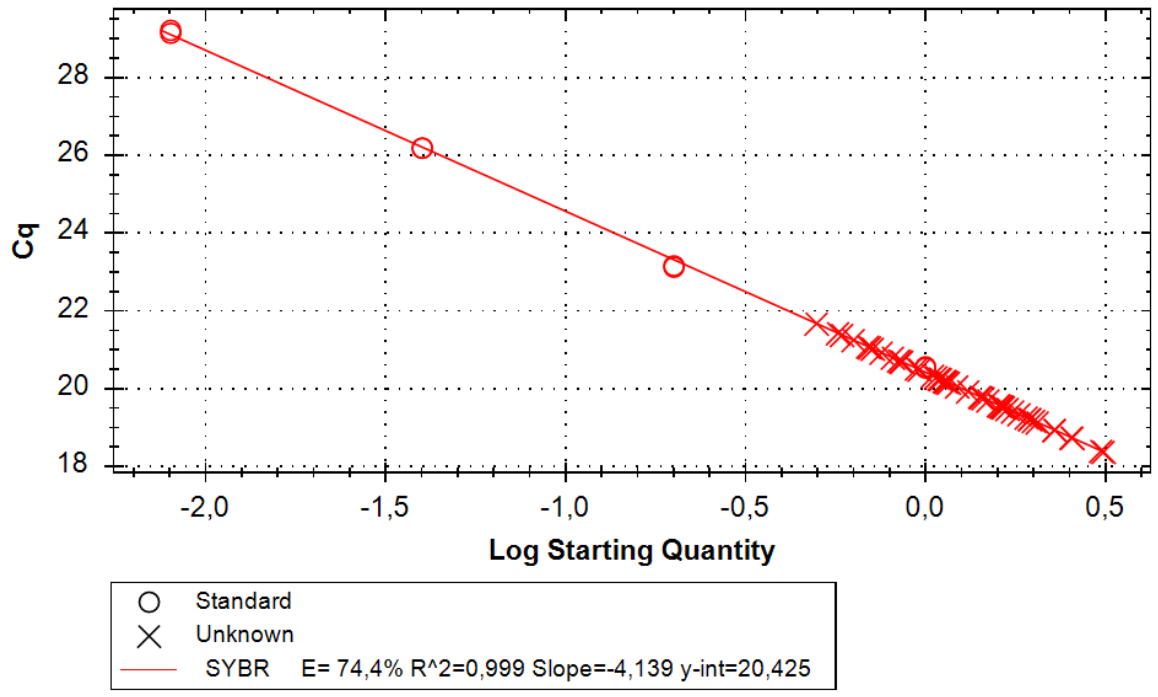

(b) Standard curve for Actin showing the linear relationship between the log starting quantity on the x-axis and the C_q values on the y-axis. The cirlces indivate the dilution series of the standard curve while the crosses are the different samples.

Figure 6: Amplification and standard curve for Actin.

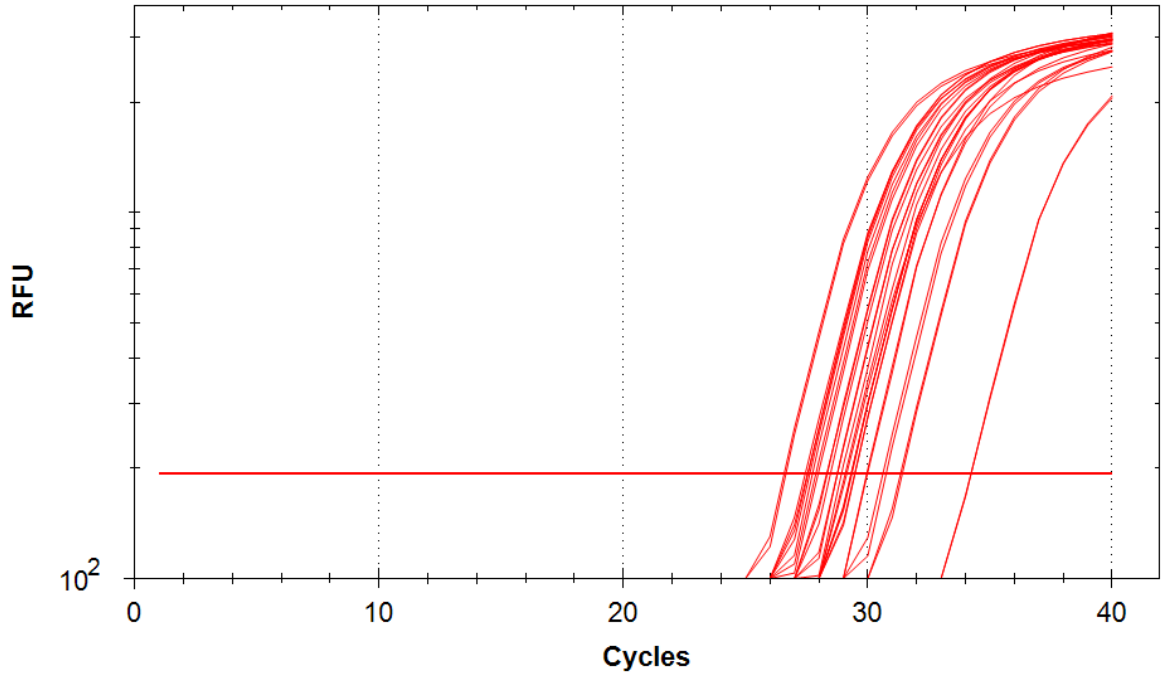

(a) Logarithmic amplification curve for PCR reaction containing hes1 primers. Amount of cycles on the x-axis and relative fluorescence unit (RFU) on the y-axis. Threshold line also displayed

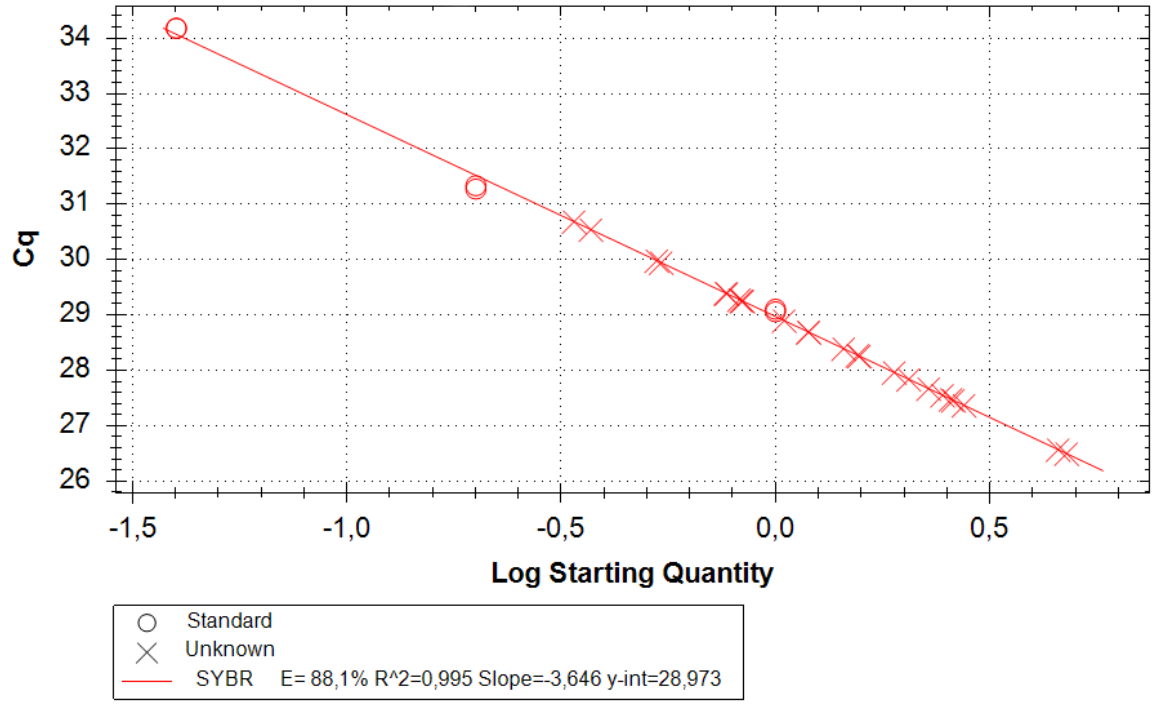

(b) Standard curve for hes1 showing the linear relationship between the log starting quantity on the x-axis and the C_q values on the y-axis. The cirlces indivate the dilution series of the standard curve while the crosses are the different samples.

Figure 7: Amplification and standard curve for Hes1.

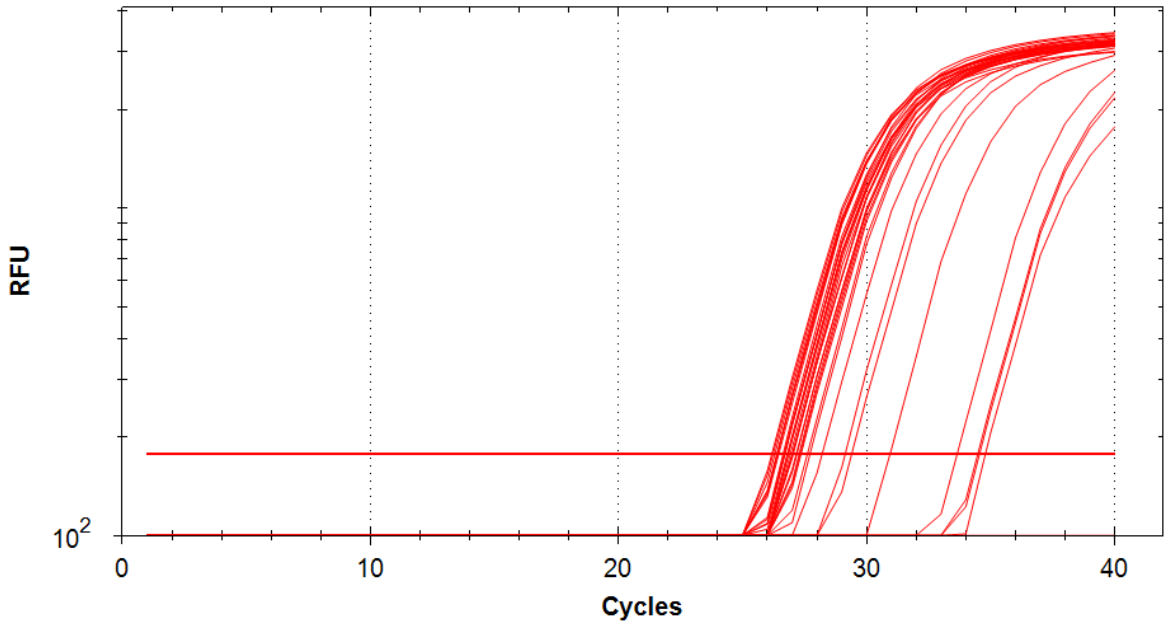

(a) Logarithmic amplification curve for PCR reaction containing FoxO1 primers. Amount of cycles on the x-axis and relative fluorescence unit (RFU) on the y-axis. Threshold line also displayed

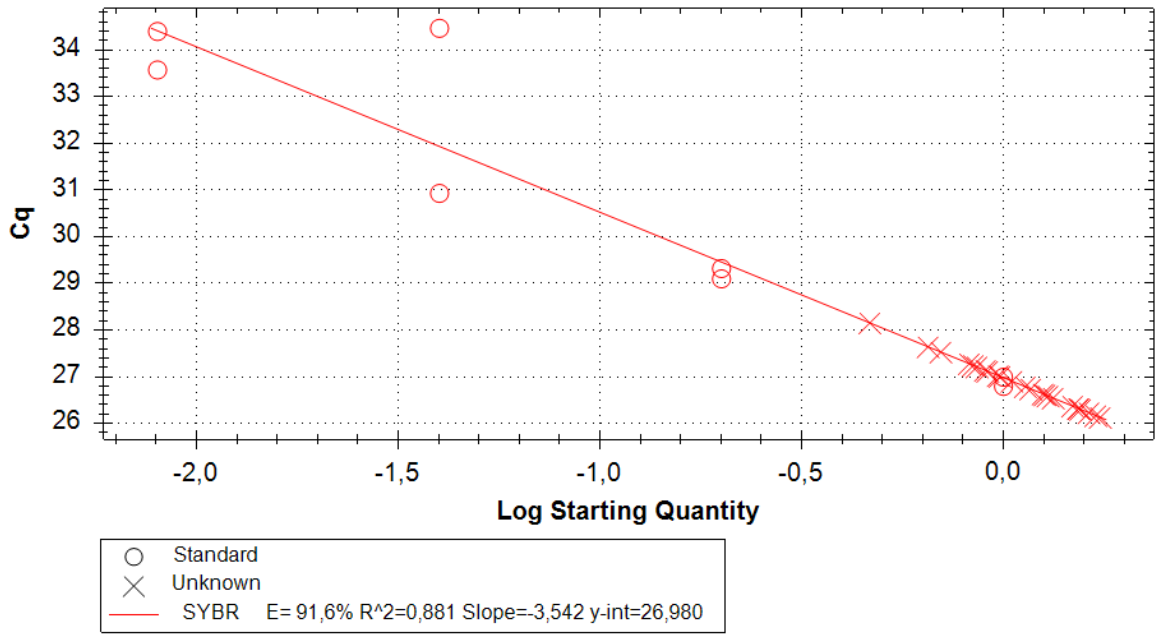

(b) Standard curve for FoxO1 showing the linear relationship between the log starting quantity on the x-axis and the C_q values on the y-axis. The cirlces indivate the dilution series of the standard curve while the crosses are the different samples.

Figure 8: Amplification and standard curve for FoxO1.

Graphs displaying the melting curves for the samples of the respective siRNAs can be found in Figure 9.

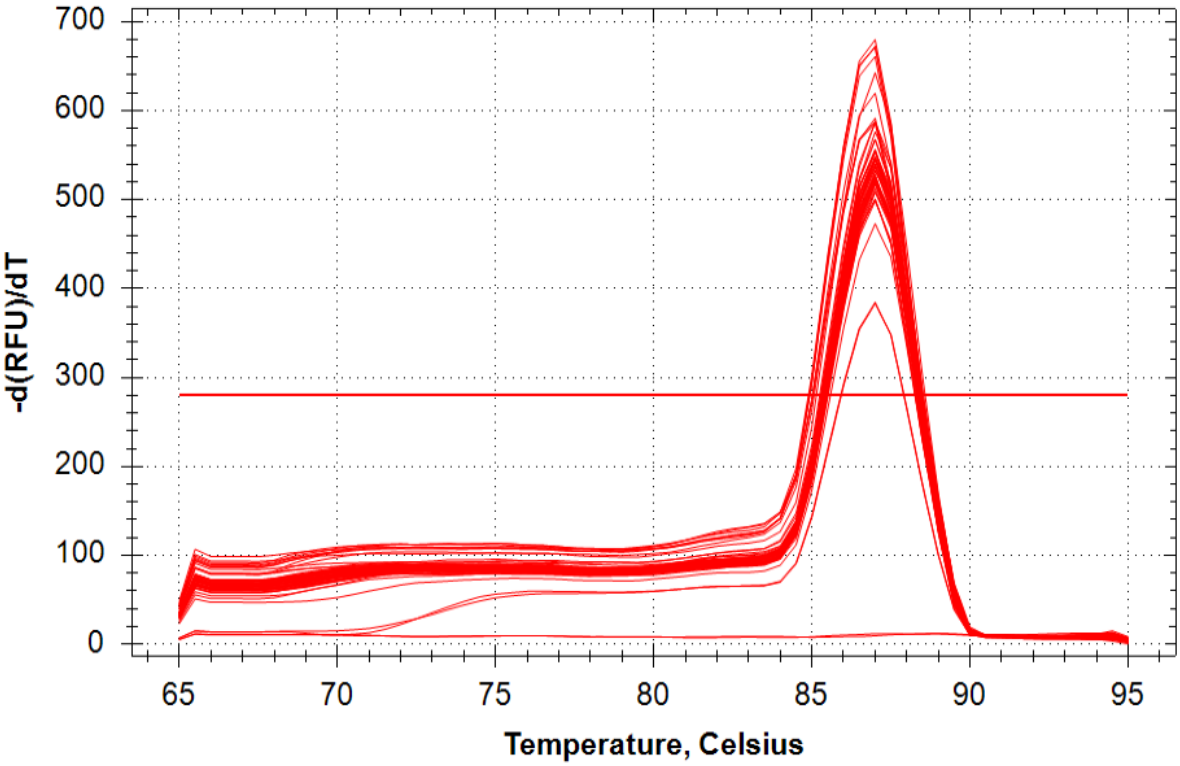

(a) Graph displaying derivative of melting curve at different temperatures for samples including Actin.

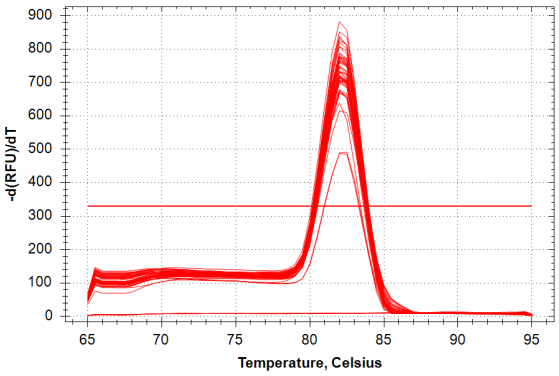

(b) Graph displaying derivative of melting curve at different temperatures for samples including Hes1.

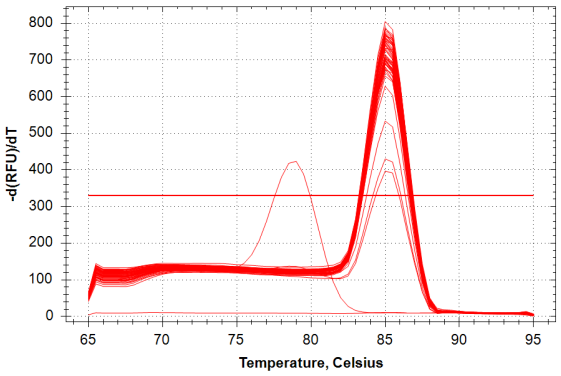

(c) Graph displaying derivative of melting curve at different temperatures for samples including FoxO1.

Figure 9: Melting curves for samples containing Actin, Hes1 and FoxO1 respectively. The x-axis shows temperature, and the y-axis the change in fluorescence.

For each sample, the expression of FoxO1 and Hes1 normalized to Actin was calculated according to the method mentioned in the method section. Figure 10 displays bar diagrams comparing the relative expression for the respective siRNAs at different time points and for Hes1 and FoxO1.

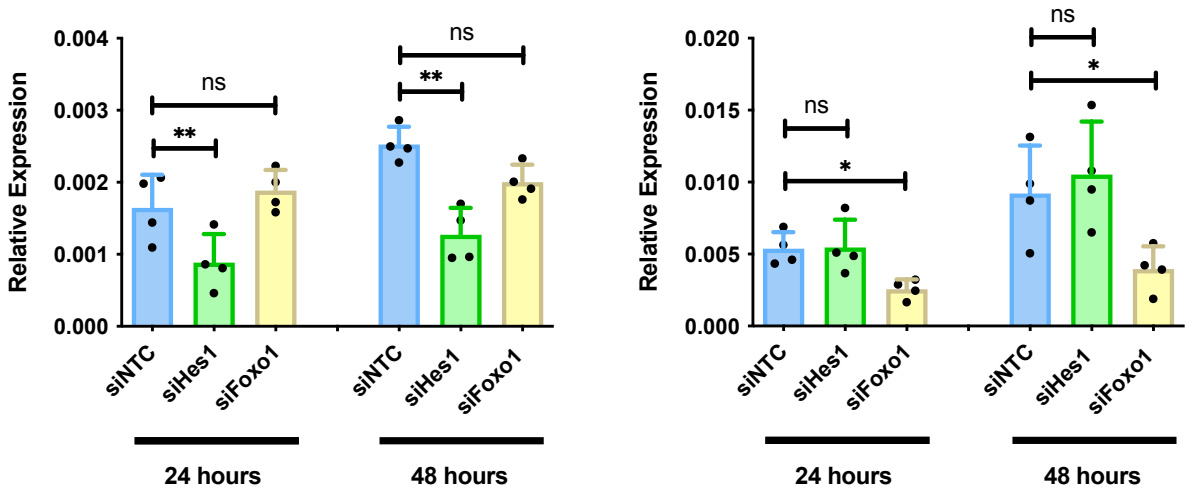

(a) Bar chart showing expression levels of Hes1 after transfection of different siRNAs for 24 and 48 hours.

(b) Bar chart showing expression levels of FoxO1 after transfection of different siRNAs for 24 and 48 hours.

Figure 10: Comparison of siRNAs impact on gene knockdown. Repeated measures one-way ANOVA was used to determine p values where * indicates $p < 0.05$ and ** implies that $p < 0.01$. Error bars indicating standard deviation and black dots represent data points.

The knockdown efficacy was determined as fold change to siNTC. This was done for the siRNAs with a significant p-value according to the RM one-way ANOVA metric. The resulting graphs can be seen in Figure 11, and the mean and standard deviation for the respective genes and time points reside in Table 6.

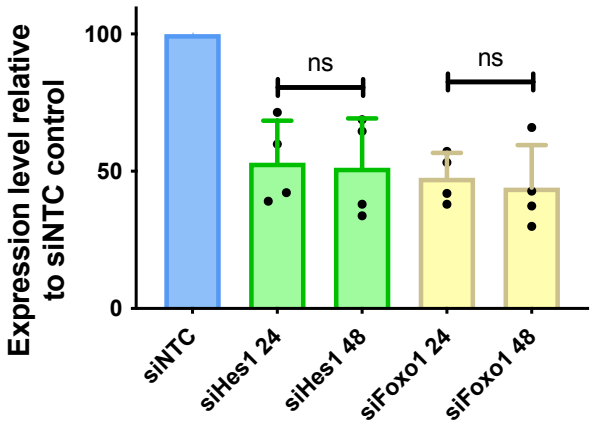

Figure 11: Comparison of relative expression normalized to siNTC and compared grouped by siRNAs. Error bars show standard deviation.

Welch's unpaired t-test was applied, assuming that the standard deviations deviated relative to each other (parametric test) and that the points followed a Gaussian distribu-

Table 6: Mean knockdown efficacy normalized to the siNTC at 24 and 48 hours for the Hes1 and FoxO1 genes. The standard deviation for all genes and time points was observed.

	24 hours	48 hours
Mean	0.47	0.49
σ	0.15	0.18

(a) Hes1

	24 hours	48 hours
Mean	0.52	0.56
σ	0.09	0.16

(b) FoxO1

tion to the adjacent bars representing the different time points for the same siRNA. The resulting p-values showcased that neither of the siRNAs showed a significant difference between the measured time points.

4 Discussion

In this study we investigated the efficacy and the duration of siRNA knockdown for the genes, Hes1 and FoxO1. The knockdown was carried out for 24 hours and the read-out was analysed using qRT-PCR after 24h and 48h from transfection start. We could observe that both genes were knocked down significantly only when the siRNA targeting for the specific gene was used. Moreover, no significant difference was seen in fold change relative to the siNTC control between the two measured time points.

Figure 10a, shows the relative expression of Hes1 and FoxO1 following siHes1 knockdown. The cells transfected with siHes1 showed a significant decrease of Hes1, which was presumed given that the knockdown was successful. A noteworthy remark is that a visual observation might conclude a decrease in the relative expression of the cDNA transfected with siFoxO1; however, an RM one-way ANOVA did not find this significant.

Figure 11 shows that after 24 hours Hes1 a obtained a 47% decrease of the fold change relative to siNTC. After 48 hours, the same expression showed a decrease of 49%. On the other hand, the fold change to siNTC yielded relatively high standard deviations of 15% and 18%, respectively. This implies a notion of uncertainty which was possibly caused by deficits in consistency for the qPCR and possible errors or contaminations during pipetting and handling of cells. This infers an irresolution that the knockdowns were precisely 47% and 49% effective, however that the knockdown was successful can be deemed conclusive.

A presumption of the exact distribution is difficult due to the limited data. In addition to this, individual cells can vary in inclination to be knocked down, and therefore ideally more samples would be analyzed.

Figure 10b showcases a significant decrease in relative expression and this implies that the gene knockdown was successful. Figure 11 and Table 6 show that the fold change in expression relative to siNTC is approximately 52% and 56% after 24 and 48 hours, respectively. The sample size was small and the data which has been observed is reasonably spread with a standard deviation of 9% and 16%, but nevertheless, the results were significant and a successful knockdown can be deemed conclusive.

Moreover, despite the uncertainty regarding the exact knockdown efficacy, an important observation concerning the knockdown duration can be made. A visual analysis might deem that for both the siHes1 and siFoxO1 the knockdown efficacy increases between 24 and 48 hours. However, this notion can be regarded as inconclusive since according to Welch's t-test, the increases were statistically not significant. This implies that no significant change of gene knockdown occurred between the time points, however further studies must be conducted to determine the exact duration of the knockdown.

Knowing the biological significance of the knockdown can not be derived merely from the knockdown efficacy. Only because a gene has been severely knocked down, an effect regarding the cellular behavior might not be observed. This is due to the previously discussed complexity of genes. Multiple genes can give rise to similar behavior which can imply that despite a gene being completely silenced, the behavior is not altered.

4.1 Validity of Results

As seen in Figure 6b, the slope of the standard curve for Actin is approximately -4.139 with an $R^2 \approx 0.999$. This implies that the curve is very well adjusted but that the qPCR efficiency is an estimated 74,4%. Ideally, the qPCR for the housekeeping gene Actin would have been repeated due to the low PCR efficiency. However, the housekeeping gene data was deemed permissible due to the other factors being very well adjusted. Furthermore, Figure 7b displays the standard curve for the Hes1 primers for a 5-fold dilution series.

The graph obtains an $R^2 \approx 0.995$ and a slope ≈ -3.646. This implies that the graph was very well adjusted to the data and that the PCR exhibited an efficiency of approximately 88.1%.

Figure 8b displays the standard curve attained using the FoxO1 primers for the 5-fold dilution series. The graph obtains an $R^2 \approx 0.881$ and a slope ≈ -3.542. These values are acceptable. However as seen on the graph, one point lies relatively far away from the graph which could have been caused by possible contamination. Removing this point would yield values of $R^2 \approx 0.984$ and a slope ≈ -3.347, which yields an efficiency of approximately 99%. However, it is noteworthy that the values can be deemed acceptable in either case.

The 260/230 values were much lower than ideal, however this is presumably since TRIzol which contains phenol was used and therefore, phenol can remain in the samples which results in high absorbance at 230 nm. The 260/280 was also lower than ideal, but not as evident as the 260/230. However, as seen in Figure 9 all the genes obtained melting curves which were by qualitative assessment deemed very good. The only inconsistency was observed for the FoxO1 melting curve where one line deviated from the remaining. This implies that generally, contamination and primer-dimer creation was low.

Another qualitative assessment which assures the validity of the results can be seen in Figure 6a, 7a and 8a. All the graphs displayed sigmoidal amplification curves, which demonstrated a shape, which were qualitatively deemed reminiscent of a theoretical approximation.

The concluding remarks is that results acquired by the experiment consisted of noteworthy deviations. However, the values were throughout the experiment deemed acceptable and the results and conclusions thereof can be interpreted as reasonable estimates.

4.2 Comparison with Previous Studies

As mentioned in the introduction, little data exists examining the gene knockdown efficacy and duration of FoxO1 and Hes1 for NSCs using lipofectamine. Studies examining the duration of HeLa cells have proclaimed a continuous consistency of gene knockdown for 5-7 days after transfection. In our study, the knockdown was only analyzed after 24 and

48 hours, but the difference in efficacy, was not deemed significant, which coincides with the HeLa cells. However siRNA transfection of HeLa cells is substantially easier than that of NSCs since HeLa cells are relatively easy to transfect due to their resilience and high reproduction speed while NSCs are substantially more fragile.

Furthermore, studies examining RNAiMAX in hES have obtained gene knockdown values of Sox2 71% and 90% for Oct4. First, it must be noted the relatively apparent difference between the two genes, which emphasizes the difference between individual genes. This is due to the different half-lives of RNA, which implies that some RNAs will be knocked down easier than others. Moreover, different cell types have different propensities to be transfected due to factors like fragility. In addition, proliferation inclination differs among cell types, implying that cells that proliferate more will give rise to daughter cells with diluted siRNA, reducing the knockdown efficiency. Consequently, even though the results in this study were lower than that of the hES, this can be deemed permissible due to the differences in genes and cell types.

Lastly, a study analyzing the transfection of NSCs initially obtained a knockdown efficacy between 40% and 77% and, after improvements, obtained an efficiency of over 80%. This further accentuates the variability in the transfection of cells, particularly it emphasizes the difference that silencing method facilitate.

Finally, in comparison with these studies, there is a degree of variation. However, it is imperative to mention that this fluctuation is not surprising due to the multitude of methods and cells used in the other experiments. Transfection method, type of cell and specific gene are all factors which impact the efficacy and duration of the silencing to an extent that comparing the efficacy of this study with the aforementioned, provides very little.

4.3 Future Studies

Understanding how genes impact NSCs is a research field that could be essential for finding treatments for MS and other neurodegenerative disorders. Consequently, obtaining an understanding of the intricacies of how gene knockdown works can be beneficial. In

this study, we took a step in that direction and examined the efficacy and duration of gene knockdown by siRNA transfection for the key regulatory genes, Hes1 and FoxO1.

Errors regarding pipetting can imply large deviations in the final result due to small alternations, especially when working with small volumes. Additionally, small flaws in equipment can likewise cause problems. The experiment was continuously dependent on equipment and slight deficits in quality could alter the results. This was exemplified by the qPCR's limited efficacy, which decreased the experiment's preciseness. To counteract this, more experiments containing more samples must be conducted to minimize uncertainty.

Furthermore, this study examined the knockdown efficacy after 24 and 48 hours. However, more time points would have to be studied to truly understand how gene knockdown varies over time. Moreover, only four samples were examined for each siRNA, and technical duplicates were only used during the PCR phase. Consequently, this increased the margin of error, and an improvement of the study would entail more samples as well as more technical duplicates. In addition to this, analyzing more genes would be beneficial for understanding more of the intricacies underlying cellular behavior. Due to the the limited samples in this study, no approximations regarding the distribution of gene knockdown efficacy could be made. However, further experiments could investigate even more samples which could determine type of distribution generated knockdown samples attain.

Furthermore, despite not being considered significant in this study, studying Hes1 behavior during the siFoxO1 transfection could give insight of how genes can impact each other. This is merely speculative, but it emphasizes that more research must be conducted in genomics.

Studies examining differences in cellular behaviour must be conducted to determine the biological significance of the results. As previously mentioned, only because the genes are knocked down, differences in behavior might not be observed. Therefore, since the theoretical efficacy of the knockdown of siRNAs has now been approximated, more studies must be conducted examining how the knockdown actually impacts the cells.

Finally, studies examining applications of regulatory genes could be beneficial. Studies could imply progress towards decreasing the severity of MS, and due to the conclusions

regarding the knockdown efficacy and duration of Hes1 and FoxO1 drawn from this study, studies utilizing the regulating properties of Hes1 and FoxO1 could be conducted.

4.4 Conclusion

The study concluded that the siRNA knockdown for Hes1 by siHes1 was approximately 47 and 49% after 24 and 48 hours, respectively. The corresponding values for siFoxO1 knockdown of FoxO1 were instead 52 and 56%. The differences in knockdown efficacy between the time points were not deemed significant in either case. Additionally, no observations of the siRNAs impacting other RNAs than the target were made. Moreover, the results contained a reasonable spread implying that the aforementioned results are presumably not the exact gene knockdown. However, the observations can still serve as approximations of the efficacy.

References

[1] J. Xiao, R. Yang, Y. Biswas, S. Zhu, Q. Xin, M. Zhang, L. Zhai, Y. Luo, X. He, C. Mao, and W. Deng, "Neural stem cell-based regenerative approaches for the treatment of multiple sclerosis.," *Molecular Neurobiology*, May 2017.

[2] Y. Takagi, "History of neural stem cell research and its clinical application," *Neurol Med Chir (Tokyo)*, Mar 2016.

[3] Yale School of Medicine, "Colón-ramos lab." `https://medicine.yale.edu/lab/colon_ramos/overview/`. Accessed: 1/7/2023.

[4] M. Elshazzly, M. Lopez, V. Reddy, and O. Caban, "Embryology, central nervous system.." `https://www.ncbi.nlm.nih.gov/books/NBK526024/`. Updated: 3/4/2023, Accessed: 30/6/2023.

[5] X. Zhao and D. L. Moore, "Neural stem cells: developmental mechanisms and disease modeling," *Cell Tissue Res*, vol. 371, pp. 1–6, Jan 2018.

[6] M. S. Vieira, A. K. Santos, R. Vasconcellos, V. A. M. Goulart, R. C. Parreira, A. H. Kihara, H. Ulrich, and R. R. Resende, "Neural stem cell differentiation into mature neurons: Mechanisms of regulation and biotechnological applications," *Biotechnol Adv*, vol. 36, pp. 1946–1970, Nov 2018.

[7] C. Gross, "Neurogenesis in the adult brain: death of a dogma," *Nature reviews neuroscience*, 2000.

[8] A. Bond, G. Ming, and H. Song, "Adult Mammalian Neural Stem Cells and Neurogenesis: Five Decades Later," *Cell press*, Oct. 2015.

[9] T. V. Johnson and K. R. Martin, *Glaucoma (second edition)*, vol. 2. Saunders Ltd., 2015.

[10] O. Gonzales-Perez, "Neural stem cells in the adult human brain," *Biol Biomed Rep*, 2012.

[11] S. Maloy and K. Hughes, *Brenner's Encyclopedia of Genetics*, vol. 2. Academic Press, 2013.

[12] S. Ro, D. Liu, H. Yeo, and J. Paik, "Foxos in neural stem cell fate decision," *Archives of Biochemistry and Biophysics*, vol. 534, pp. 55–63, 2013.

[13] Y. Nakamura, S. Sakakibara, T. Miyata, M. Ogawa, T. Shimazaki, S. Weiss, R. Kageyama, and H. Okano, "The bhlh gene hes1 as a repressor of the neuronal commitment of cns stem cells," *Journal of Neuroscience*, vol. 20, pp. 283–293, 2000.

[14] M. M. Goldenberg, "Multiple Sclerosis Review," *Pharmacy and Therapeutics*, Mar. 2012.

[15] N. Ghasemi, S. Razavi, and E. Nikzad, "Multiple sclerosis: Pathogenesis, symptoms, diagnoses and cell-based therapy," *Cell Journal*, vol. 19, no. 1, pp. 1–10, 2017.

[16] T. Olsson, C. Barcellos, and L. Alfredsson, "Interactions between genetic, lifestyle and environmental risk factors for multiple sclerosis," *Nature reviews neurology*, Dec 2016.

[17] A. Genchi, E. Brambilla, F. Sangalli, M. Radaelli, M. Bacigaluppi, R. Furlan, A. Andolfo, D. Drago, C. Magagnotti, G. M. Scotti, R. Greco, P. Vezzulli, L. Ottoboni, M. Bonopane, D. Capilupo, F. Ruffini, D. Belotti, B. Cabiati, S. Cesana, G. Matera, L. Leocani, V. Martinelli, L. Moiola, L. Vago, P. Panina-Bordignon, A. Falini, F. Ciceri, A. Uglietti, M. P. Sormani, G. Comi, M. A. Battaglia, M. A. Rocca, L. Storelli, E. Pagani, G. Gaipa, and G. Martino, "Neural stem cell transplantation in patients with progressive multiple sclerosis: An open-label, phase 1 study," *Nature Medicine*, vol. 29, pp. 75–85, January 2023.

[18] J. Starega-Roslan, P. Galka-Marciniak, and W. J. Krzyzosiak, "Nucleotide sequence of mirna precursor contributes to cleavage site selection by dicer," *Nucleic Acids Research*, vol. 43, no. 22, pp. 10939–10951, 2015.

[19] H. O. Iwakawa and Y. Tomari, "Life of RISC: Formation, action, and degradation of RNA-induced silencing complex," *Mol Cell*, vol. 82, pp. 30–43, Jan 2022.

[20] H. Dana, G. M. Chalbatani, H. Mahmoodzadeh, R. Karimloo, O. Rezaiean, A. Moradzadeh, N. Mehmandoost, F. Moazzen, A. Mazraeh, V. Marmari, M. Ebrahimi, M. M. Rashno, S. J. Abadi, and E. Gharagouzlo, "Molecular Mechanisms and Biological Functions of siRNA," *Int J Biomed Sci*, vol. 13, pp. 48–57, Jun 2017.

[21] Y. Zhang, *RNA-induced Silencing Complex (RISC)*, pp. 1876–1876. New York, NY: Springer New York, 2013.

[22] M. Carter and J. Shieh, *Guide to Research Techniques in Neuroscience*, vol. 2. Academic Press, 2015.

[23] M. Zhao, H. Yang, X. Jiang, W. Zhou, B. Zhu, Y. Zeng, K. Yao, and C. Ren, "Lipofectamine RNAiMAX: an efficient siRNA transfection reagent in human embryonic stem cells," *Mol Biotechnol*, vol. 40, pp. 19–26, Sep 2008.

[24] ThermoFischer, "Glycoblue™ coprecipitant (15 mg/ml)." `https://www.thermofisher.com/order/catalog/product/AM9516`. Accessed: 4/7/2023.

[25] D. C. Rio, M. Ares, G. J. Hannon, and T. W. Nilsen, "Purification of RNA using TRIzol (TRI reagent)," *Cold Spring Harb Protoc*, vol. 2010, Jun 2010.

[26] B. Matlock, "Assessment of nucleic acid purity," *Thermo Fischer Scientific*, 2012.

[27] S. Spiegleman and D. L. Watson, K. F. Kacian, "Synthesis of complementary dna," *Proc. Natl. Acad. Sci. U.S.A.*, vol. 68, pp. 2843–2845, 1971.

[28] A. Manit, S. S. Iqbal, M. Williamson, L. Gommersall, N. Arya, and H. Patel, "Basic principles of real-time quantitative pcr," *Journal of Neuroscience Methods*, vol. 209, no. 2, pp. 420–427, 2005.

[29] National Library of Medicine, "Polymerase chain reaction (pcr)." `https://www.ncbi.nlm.nih.gov/probe/docs/techpcr/`. Accessed: 10/7/2023.

[30] D. J. P. G. Rocha, T. L. P. Castro, E. R. G. R. Aguiar, and L. G. C. Pacheco, *Real-time PCR*, vol. 2. Humana Press, 2006.

[31] T. Dorak, ed., *Real-time PCR*. Taylor & Francis, 2006.

[32] ThermoFischer, "Efficiency of real-time pcr." https://www.thermofisher.com/us/en/home/life-science/pcr/real-time-pcr/real-time-pcr-learning-center/real-time-pcr-basics/efficiency-real-time-pcr-qpcr.html. Accessed: 10/7/2023.

[33] ThermoFischer, "Poor efficiency of pcr." https://www.thermofisher.com/se/en/home/life-science/pcr/real-time-pcr/real-time-pcr-learning-center/real-time-pcr-basics/real-time-pcr-troubleshooting-tool/gene-expression-quantitation-troubleshooting/poor-pcr-efficiency.html. Accessed: 8/7/2023.

[34] ThermoFischer, "Rna interference (rnai) is an evolutionarily conserved mechanism for silencing gene expression." `https://www.thermofisher.com/se/en/home/references/ambion-tech-support/rnai-sirna/tech-notes/duration-of-sirna-induced-silencing.html`. Accessed: 3/7/2023.

[35] B. Bertram, S. Wiese, and A. von Holst, "High-efficiency transfection and survival rates of embryonic and adult mouse neural stem cells achieved by electroporation," *Journal of Neuroscience Methods*, vol. 209, no. 2, pp. 420–427, 2012.

A Appendix

The following tables include data regarding the experiment conducted.

Table 7: During the seeding of the cells, all the cultures were supposed to have 75 000 cells and an equal volume. Table shows the volume of cells which were used for each cell culture to ensure an equal amount of cells in each petri dish.

Index	Concentration [cells/mL]	Volume [µL]
1	1.6×10^6	46.9
2	1.4×10^6	53.6
3	2.1×10^6	35.7
4	1.8×10^6	41.7

Table 8: RNA concentration generated by the spectrophotometer and designated amount to add to the tubes before cDNA conversion for 24 hour RNA.

Sample	Concentration [ng/µL]	RNA solution [µL]	RNase-free water [µL]
siNTC 1	38.1	13.9	1.1
siNTC 2	57.0	9.3	5.7
siNTC 3	79.1	6.7	8.3
siNTC 4	58.7	9.0	6.0
siHes1 1	46.2	11.5	3.5
siHes1 2	64.2	8.2	6.8
siHes1 3	49.6	10.7	4.3
siHes1 4	64.9	8.2	6.8
siFoxo1 1	59.5	8.9	6.1
siFoxo1 2	61	8.7	6.3
siFoxo1 3	58.1	9.1	5.9
siFoxo1 4	58.6	9.0	6.0
siTcf7l2 1	45.6	11.6	3.4
siTcf7l2 2	35.3	15.0	0.0
siTcf7l2 3	40.9	12.9	2.1
siTcf7l2 4	41.3	12.8	2.2

Table 9: RNA concentration generated by the spectrophotometer and designated amount to add to the tubes before cDNA conversion for 48 hour RNA.

Sample	Concentration [ng/µL]	RNA solution [µL]	RNase-free water [µL]
siNTC 1	84.1	4.4	10.6
siNTC 2	80.9	4.5	10.5
siNTC 3	128.9	2.9	12.1
siNTC 4	51.6	7.1	7.9
siHes1 1	58.6	6.3	8.7
siHes1 2	52.4	7.0	8.0
siHes1 3	48.2	7.6	7.4
siHes1 4	55.7	6.6	8.4
siFoxo1 1	47.5	7.7	7.3
siFoxo1 2	36.4	10.1	4.9
siFoxo1 3	24.8	14.8	0.2
siFoxo1 4	32.0	11.5	3.5
siTcf7l2 1	30.0	12.3	2.8
siTcf7l2 2	24.5	15,0	0.0
siTcf7l2 3	30.2	12.2	2,8
siTcf7l2 4	49,1	7.5	7.5

Table 10: 260/280 and 260/280 ratios for different siRNAs after 24 hours

siRNA	260/280	260/230
siNTC 1	1.57	0.48
siNTC 2	1.5	0.25
siNTC 3	1.58	0.62
siNTC 4	1.57	0.31
siHes1 1	1.49	0.25
siHes1 2	1.5	0.55
siHes1 3	1.55	0.29
siHes1 4	1.53	0.41
siFoxo1 1	1.52	0.43
siFoxo1 2	1.5	0.42
siFoxo1 3	1.44	0.57
siFoxo1 4	1.42	0.55

Table 11: RNA concentration generated by the spectrophotometer and designated amount to add to the tubes before cDNA conversion for 48 hour RNA.

Primer	Sequence
mActinF	5'-TGGAATCCTGTGGCATCCATGAAAC-3'
mActinR	5'-TAAAACGCAGCTCAGTAACAGTCCG-3'
mFoxo1F	5'-GTCGTTTCTGCTGTGATTCC-3'
mFoxo1R	5'-CACTTGGATTGAGGACCACTT-3'
mHes1F	5'-ACACCGGACAAACCAAAGAC-3'
mHes1R	5'-ATGCCGGGAGCTATCTTTCT-3'